Supporting Information

Proton and Copper Binding to Humic Acids Analyzed by XAFS Spectroscopy and Isothermal Titration Calorimetry

Jinling Xu,[†,‡] Luuk K. Koopal,[§,‖] Linchuan Fang,*[,†] Juan Xiong,[§] and Wenfeng Tan*[,†,§]

[†] State Key Laboratory of Soil Erosion and Dryland Farming on the Loess Plateau, Institute of Soil and Water Conservation, Chinese Academy of Sciences and the Ministry of Water Resources, Yangling, Shaanxi Province 712100, P. R. China

[‡] University of Chinese Academy of Sciences, Beijing, 100049, P. R. China

[§] College of Resources and Environment, Huazhong Agricultural University, Wuhan 430070, P. R. China

[‖] Physical Chemistry and Soft Matter, Wageningen University and Research, Stippeneng 4, 6708 WE Wageningen, The Netherlands

* Corresponding authors
flinc629@hotmail.com and wenfeng.tan@hotmail.com

Contents page

Non-Ideal Competitive Adsorption (NICA) Model ……S2
Table S1 ……..S4
Figure S1 ……S5
Figure S2 ……S5
Intrinsic and Conditional Affinity Distributions…….S6
Figure S3 ……S7
Sample Preparation and Data Collection for XAFS Spectra……..S8
Figure S4 ……S9
Figure S5 ……S10
Figure S6 ……S11
Table S2 ……..S12
Table S3 ……..S13
Table S4 ……..S14
Figure S7 ……S15
Figure S8 ……S16
References……...S17

Non-Ideal Competitive Adsorption (NICA) Model

An outline of the NICA model is presented, more details on the derivation of the NICA model can be found in refs[1, 2] and discussions of the application of the NICA model in combination with a model for the electrostatic interactions, the NICA-Donnan model, can be found in refs[3-5]. The NICA model is a simplification of the NICA-Donnan model; it does not explicitly consider the electrostatic interactions. To a good approximation this simplification applies well at relatively high ionic strength, say ≥ 0.1 M, where the electrostatic interactions are relatively small. The NICA model is based on site binding and the overall non-ideality is divided into heterogeneity of the binding sites (property of the humic substance) and an ion-specific non-ideality (stoichiometry of the binding). The binding site heterogeneity is considered on the basis of continuous distributions of affinities. Proton binding studies on HS have revealed that for ion binding to humic substances two main types of sites, often described as “carboxylic-type” (low proton affinity) and “phenolic-type” (high proton affinity) that each are heterogeneous, have to be considered.[6] As the electrostatic interactions are not taken into account explicitly in NICA model and they become part of the affinity distributions. The expression of the NICA equation for specific binding of cation *i* to each of the two site types *j* (1: carboxylic; 2: phenolic) is

$$\theta_{i,j} = \frac{\left(\tilde{k}_{i,j} c_i\right)^{n_{i,j}}}{\sum_i \left(\tilde{k}_{i,j} c_i\right)^{n_{i,j}}} \times \frac{\left[\sum_i \left(\tilde{k}_{i,j} c_i\right)^{n_{i,j}}\right]^{p_j}}{1 + \left[\sum_i \left(\tilde{k}_{i,j} c_i\right)^{n_{i,j}}\right]^{p_j}} \qquad \text{(S1)}$$

where $\theta_{i,j}$ is the fraction of site-type j occupied by ion i, $\tilde{k}_{i,j}$ the mode (peak) of the affinity distribution of species i for site-type j, $n_{i,j}$ the *average* site-type-specific non-ideality (stoichiometry) of ion i in relation to sites of type j, p_j ($0 < p_j \leq 1$) the generic width of the affinity distribution of site type j and c_i the concentration of ion i. For the determination of the maximum amounts of sites of type 1 and 2, the proton (H) binding isotherm is used. The total amount of bound ion i, $Q_{i,j}$, to site-type j is then given by

$$Q_{i,j} = \theta_{i,j}\left(\frac{n_{i,j}}{n_{\mathrm{H},j}}\right)Q_{\max \mathrm{H},j} \tag{S2}$$

where $Q_{\mathrm{maxH},j}$ is the maximum site density of site-type j, as observed with proton binding (H refers to proton). The factor $n_{i,j}/n_{\mathrm{H},j}$ denotes the average stoichiometry of metal ion i bound to site-type j using the average proton stoichiometry as reference. The product $(n_{i,j}/n_{\mathrm{H},j})Q_{\mathrm{maxH},j}$ expresses that, due to differences in stoichiometry of H and i for binding sites j, the maximum binding of i on sites j is also different from that of H on sites j.

For proton binding, the eq S1 can be simplified as

$$\theta_{\mathrm{H},j} = \frac{\left(\tilde{k}_{\mathrm{H},j}c_{\mathrm{H}}\right)^{m_{\mathrm{H},j}}}{1+\left(\tilde{k}_{\mathrm{H},j}c_{\mathrm{H}}\right)^{m_{\mathrm{H},j}}} \tag{S3}$$

where $m_{\mathrm{H},j} = n_{\mathrm{H},j} \times p_j$. As proton binding can be studied in the absence of site competition, the parameter $m_{\mathrm{H},j}$ characterizes the overall non-ideality of proton binding to sites of type j; when it is assumed that $n_{\mathrm{H},j} = 1$ the overall non-ideality reduces to a non-ideality due to site heterogeneity.

The binding of heavy metal ion *i* can only be studied in the presence of protons and in that case the combined knowledge of proton binding and heavy metal ion binding allows the determination of the two *generic* site-type-specific distribution functions (characterized by the p_j values that apply to all ion types) and the ion-specific parameters $n_{i,j}$ and $n_{H,j}$ that are consistent with the generic distribution functions. The combined information on multicomponent ion binding thus allows for each site-type the separation of the binding non-ideality in a generic heterogeneity effect and ion-specific stoichiometry effects.

Table S1. NICA Model Parameters of Proton and Cu Binding to JLHA and PAHA in 0.1 mol/L KNO_3

	JLHA	PAHA
$Q_{maxH,1}$	4.46	2.97
m_{H1}	0.36	0.48
$\log\tilde{k}_{H,1}$	4.47	4.66
n_{H1}	0.73	0.80
n_{Cu1}	0.49	0.48
n_{Cu1}/n_{H1}	0.67	0.60
$\log\tilde{k}_{Cu,1}$	3.82	4.65
p_1	0.49	0.60
$Q_{maxH,2}$	1.38	2.86
m_{H2}	0.60	0.22
$\log\tilde{k}_{H,2}$	9.31	9.21
n_{H2}	0.81	0.61
n_{Cu2}	0.41	0.43
n_{Cu2}/n_{H2}	0.51	0.70

$\log\tilde{k}_{Cu,2}$	8.26	8.55
p_2	0.74	0.36

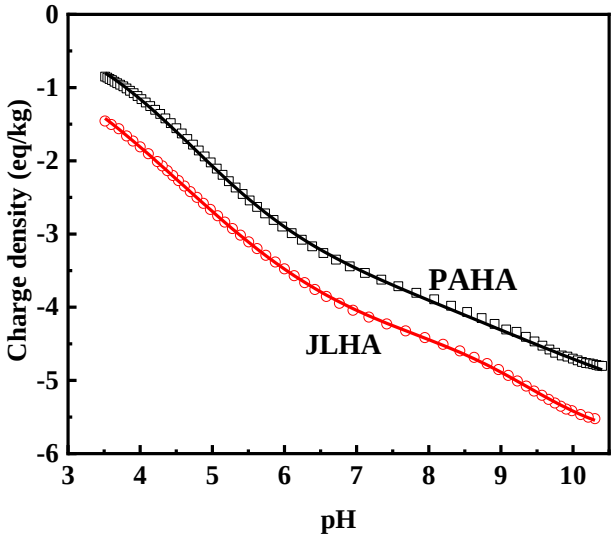

Figure S1. Charge density (eq/kg) due to proton dissociation as a function of pH for JLHA and PAHA in 0.1 mol/L KNO_3. Symbols represent the experimental data, which are from Tan et al.[7]; lines the results obtained by fitting the NICA model to the data.

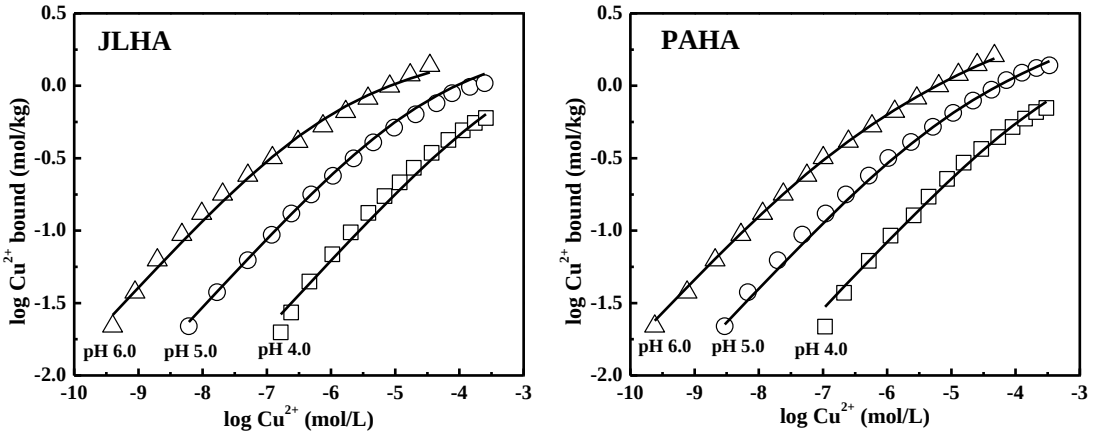

Figure S2. Copper binding to JLHA and PAHA at pH 4.0, 5.0, and 6.0 in 0.1 mol/L KNO_3 as a function of equilibrium concentration of Cu^{2+}. Symbols represent experimental data that are from Xu et al.[8], curves are obtained by fitting the NICA model to the data.

Intrinsic and Conditional Affinity Distributions

The NICA parameters in Table S1 reflect the (semi)intrinsic binding properties of HAs (I = 0.1 mol/L); the intrinsic affinity parameters imply that dissociated phenolic groups have larger affinity for Cu than dissociated carboxylic groups. However, in practice the groups are not fully dissociated, the binding occurs at a given pH and H^+ will compete with Cu^{2+} for the HA sites. Since phenolic-type sites have also a high affinity for H^+ binding (see Table S1), the *conditional* affinity (at a given pH) for Cu is lower; for the "low affinity" carboxylic-type sites the *conditional* affinity for Cu also shifts, but less than for the phenolic sites. The situation is illustrated in Figure S3 that depicts the calculated *intrinsic* (red curves) and *conditional* (blue curves) affinity distributions at pH 5.0. It follows that at pH 5.0, the conditional distribution of the phenolic-type sites has lower affinities for Cu than the conditional distribution of the carboxylic-type sites. Therefore, at pH 5.0 Cu binding preferentially takes place on the carboxylic-type sites.

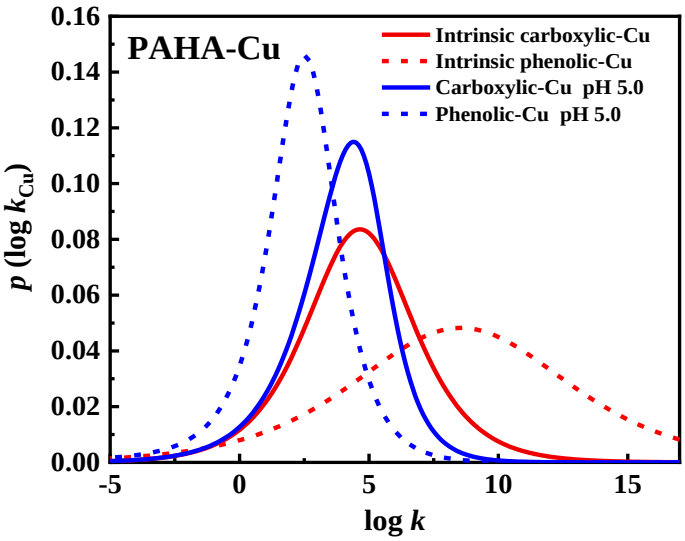

Figure S3. Comparison of the intrinsic and conditional affinity distributions of Cu binding to the carboxylic- and phenolic-type sites. The red curves represent the *intrinsic* affinity distributions of Cu binding to (dissociated) carboxylic- (solid curve) and (dissociated) phenolic-type (dashed curve) sites. The blue curves represent the *conditional* affinity distributions of Cu binding to the carboxylic- (solid curve) and phenolic-type sites (dashed curve) at pH 5.0 where the groups are partly in the protonated form.

Sample Preparation and Data Collection for XAFS Spectra

Humic acid-Cu samples for the XAFS analysis were prepared by adding 12.75 mL 0.01 mol/L $Cu(NO_3)_2$ solution gradually to 60 mL of 0.8 g/L HA at pH 6.0 in 0.1 mol/L KNO_3. During the addition the HA solution was stirred and after the addition the pH was readjusted to 6.0 by adding 0.025 mol/L KOH and the solution was equilibrated for 6 h. This procedure leads a bound amount of Cu of about 1.9 mol/kg for the HAs; a high bound amount was selected in order to obtain reliable XAFS information. Then the HA-Cu solutions were filtered through a 0.45 μm polyethylene membrane filter with a diameter of 25 mm to collect the Cu-HA complexes on the filter. The thick paste on the filter was washed twice with 0.1 mol/L KNO_3 (pH 6.0) to remove non-adsorbed Cu. The wet paste was used to collect the XAFS spectra.

Copper *K*-edge X-ray absorption spectra of the HA-Cu samples and reference materials were measured at room temperature on the 1W1B beamline at the Beijing Synchrotron Radiation Facility (BSRF). The electron beam energy was 2.5 GeV, with a maximum beam current of 250 mA. The monochromator consisted of two parallel Si (111) crystals with a resolution of 1 to 3×10^{-4} eV. The photon flux was above 4×10^{11} phs/s and the beam size on the sample was maintained at 0.9 mm × 0.3 mm. A Cu foil internal reference was used with the first inflection point set at 8979.0 eV to calibrate the X-ray energies. The XAFS spectra for HA-Cu samples and the 0.01 mol/L $Cu(NO_3)_2$ solution (reference) were collected using the fluorescence mode; the CuO powder (reference) was measured in the transmission mode.

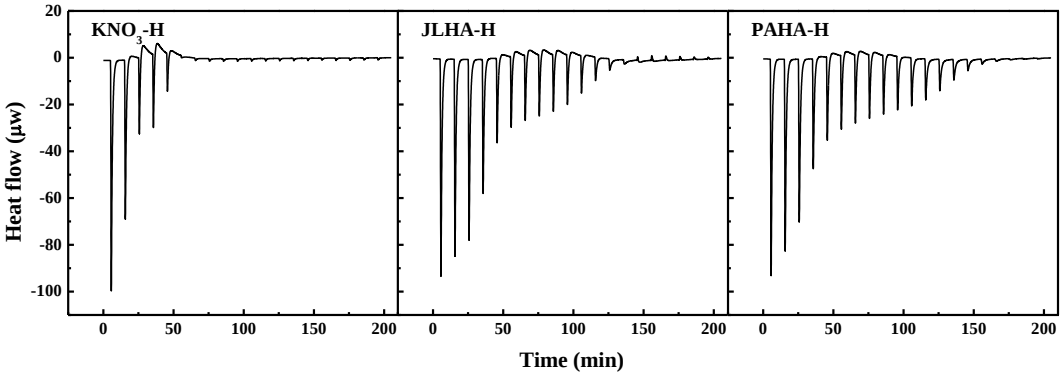

Figure S4. Basic result of the ITC measurements: heat flow released per injection of 0.028 mol/L HNO_3 into 0.1 mol/L KNO_3 (blank) and into the 0.8 g/L HA solutions with 0.1 mol/L KNO_3.

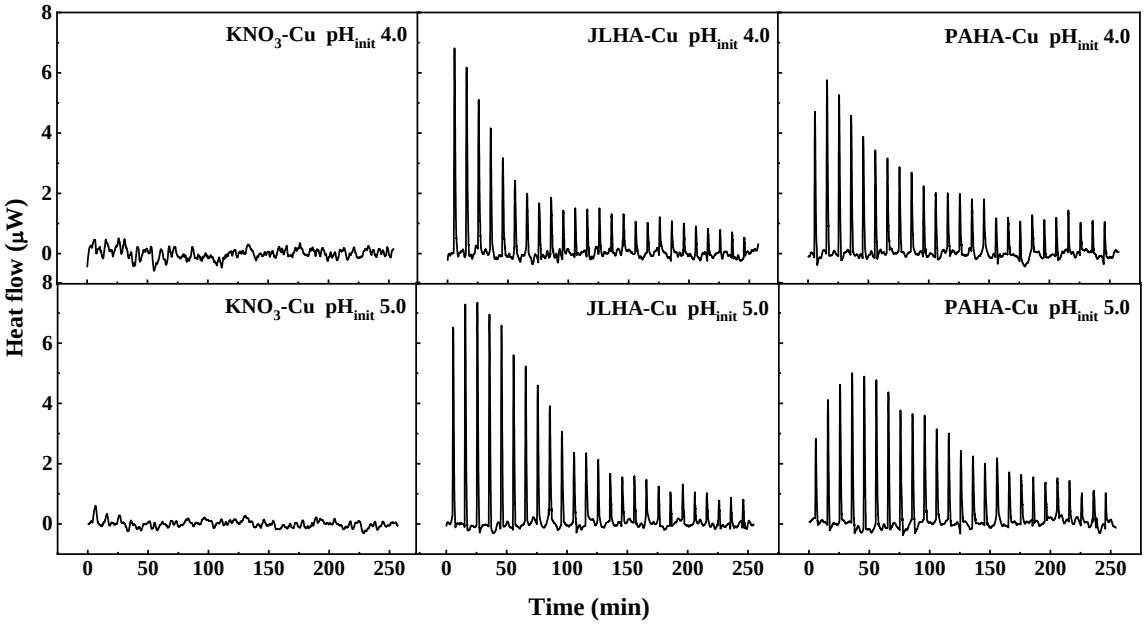

Figure S5. Basic result of the ITC measurements: heat flow released per injection of 5 mmol/L $Cu(NO_3)_2$ into 0.1 mol/L KNO_3 (blank) and into the 0.8 g/L HA solutions with 0.1 mol/L KNO_3.

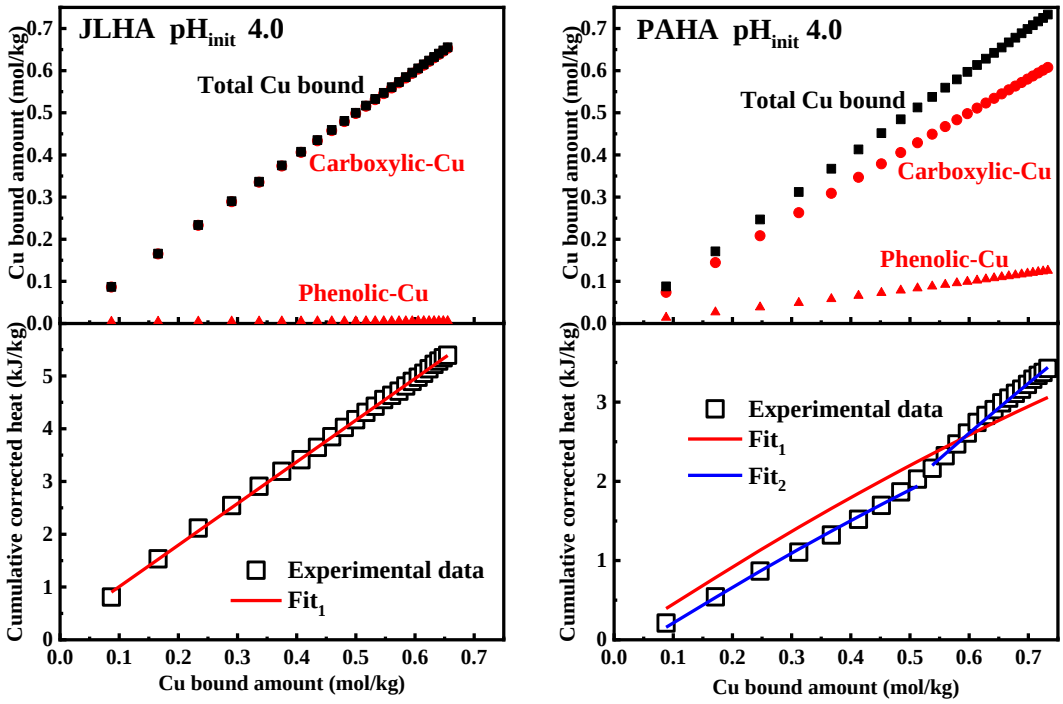

Figure S6. Comparison of the adsorption and heat characteristics of JLHA and PAHA at initial pH 4.0 in 0.1 mol/L KNO_3. The top panels depict the bound amounts of carboxylic-Cu (solid red spheres), phenolic-Cu (solid red triangles), and total Cu bound (solid black squares) and the bottom panels the cumulative heat corrected by the heat of background and proton exchange (open black squares) as a function of the total amount of Cu^{2+} bound to JLHA and PAHA. The symbols in the bottom panels are the experimental data; the red lines are data fitted (Fit_1) with eq 3. The blue lines (Fit_2) are refined data fitted with eq 3 that are fitted by making a difference between low and high Cu loadings.

Table S2. Thermodynamic Parameters for H Binding to Low Molar Mass Organic Acids at 25 ^{o}C (Data from Smith et al.[9])

ligand	site	log *K*	ΔG (kJ/mol)	ΔH (kJ/mol)	$T\Delta S$ (kJ/mol)	ionic strength
acetic acid	-COOH	4.56	–26.0	–0.41	25.5	0.1
propionic acid	-COOH	4.87	–27.2	0.75	28.6	0.0
oxalic acid	$-COOH_{(1)}$	3.82	–21.8	6.02	27.8	0.1
	$-COOH_{(2)}$	1.2	–6.8	2	9.5	0.1
malonic acid	$-COOH_{(1)}$	5.27/5.39	–30.1/–30.7	4.64/3.8	33.7/34.6	0.1
	$-COOH_{(2)}$	2.65/2.68	–15.1/–15.3	–0.29/–2.2	13.0/14.8	0.1
benzoic acid	-COOH	4.0	–22.9	–0.75	22.2	0.1
succinic acid	-COOH	2.98	–15.0	2.9	17.9	1
phthalic acid	$-COOH_{(1)}$	4.9/5.1	–28.1/–30.0	0.83	29.8	0.1
	$-COOH_{(2)}$	2.8	–15.8	1.2	17.0	0.1
salicylic acid	-OH	13.4	–76.5	–35.7~–38.0	37.6~42.3	0.0~1.0
	-COOH	2.8	–16.0	–3.8	11.9	0.1
phenol	-OH	9.8	–55.9	–24.6	31.0	0.1
catechol	$-OH_{(1)}$	13.3	–75.9	–20	54.8	0.1
	$-OH_{(2)}$	9.3	–52.8	–25	27.7	0.1

K refers to the affinity constant.

Table S3. Thermodynamic Parameters for Cu Binding to Low Molar Mass Organic Acids at 25 ^{o}C (Data from Smith et al.[9])

ligand	formula	log *K*	*ΔH* (kJ/mol)	*TΔS* (kJ/mol)	ionic strength
acetic acid (HL)	[ML]/[M][L]	2.21~1.67	7.1~5.4	19.7~15.0	0.0~1.0
propionic acid (HL)	[ML]/[M][L]	1.7	4.1	13.8	1.0
2-furoic acid (HL)	[ML]/[M][L]	1.1	4.6	10.7	1.0
succinic acid	[ML]/[M][L]	2.7	11	26.7	0.1
(H_2L)	[MHL]/[M][HL]	1.8	2	12.8	0.1
malonic acid	[ML]/[M][L]	5.04	5.8	34.6	0.1
(H_2L)	[MHL]/[M][HL]	2.08	–0.4	11.3	0.1
	$[ML_2]/[M][L]^2$	7.8	5	49.5	0.1
methylmalonic acid	[ML]/[M][L]	4.89	9.2	37.0	0.1
(H_2L)	[MHL]/[M][HL]	1.66	–	–	0.1
	$[ML_2]/[M][L]^2$	7.49	10	53.3	0.1
benzoic acid (HL)	[ML]/[M][L]	1.6	–	–	0.1
phenylacetic acid (HL)	[ML]/[M][L]	1.75	–	–	0.1
phthalic acid	[ML]/[M][L]	3.22	10	28.8	0.1
(H_2L)	[MHL]/[M][HL]	1.3	1	8.9	0.1
	$[ML_2]/[M][L]^2$	5.5	15	46.8	0.1
salicylic acid (H_2L)	[ML][H]/[M][HL]	–2.8/ [a]4.2	17	0.4	0.5
catechol (H_2L)	$[ML][H]^2/[M][H_2L]$	–8.39/ [a]5.6	13	–34.7	0.1
	[MHL]/[ML][H]	0.85	–20	–16.1	0.1

[a]Data are the values from Cabaniss et al.[10]. *K* represents the affinity constant. M refers to Cu^{2+}. L, HL and H_2L refer to the ligand with none, one and two proton(s), respectively.

Table S4. Site-type-specific Average Molar Enthalpies for Cu Binding to HA at pH_{init} 4.0 and 5.0 in 0.1 mol/L KNO_3

sample	pH_{init}	species	$\bar{\Delta H_j}$ (kJ/mol)	R^2
JLHA	4.0	carboxylic-Cu	7.95	0.999
		phenolic-Cu	28.03	
	5.0	carboxylic-Cu	8.32	0.999
		phenolic-Cu	26.63	
PAHA	4.0	carboxylic-Cu	8.74	0.993
		phenolic-Cu	11.78	
	refined	carboxylic-Cu_{low}	7.37	0.998
		phenolic-Cu_{low}	11.86	
		carboxylic-Cu_{high}	10.95	0.999
		phenolic-Cu_{high}	11.39	
	5.0	carboxylic-Cu	6.22	0.992
		phenolic-Cu	11.73	
	refined	carboxylic-Cu_{low}	5.08	0.998
		phenolic-Cu_{low}	11.44	
		carboxylic-Cu_{high}	8.88	0.999
		phenolic-Cu_{high}	11.96	

The refined values are the enthalpies fitted by making a difference between low and high Cu loadings.

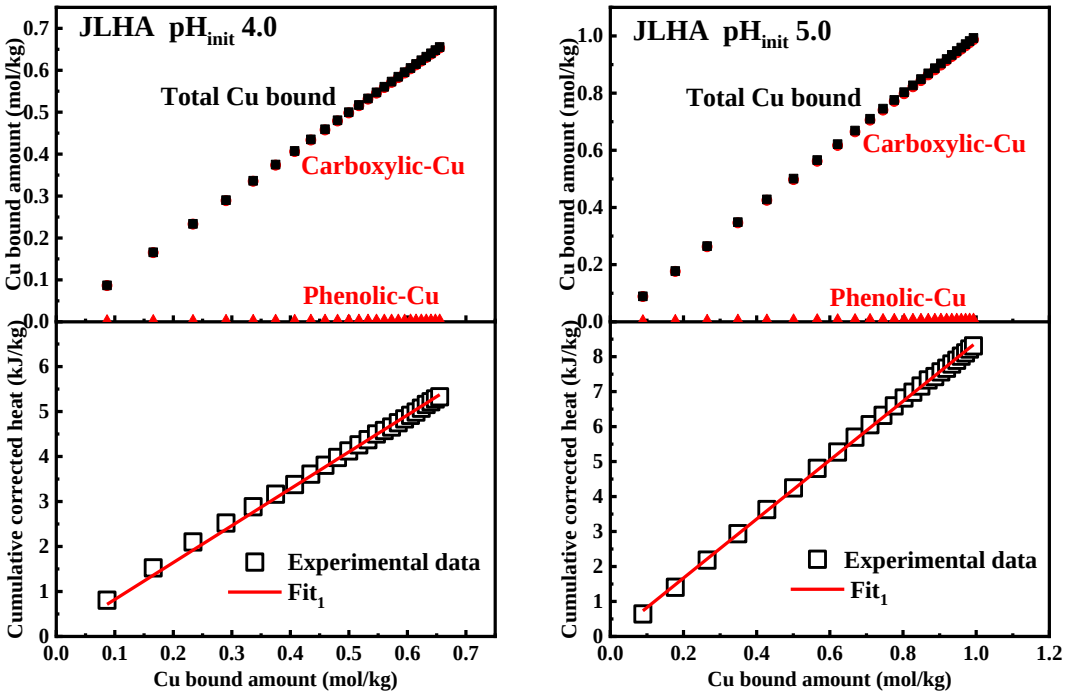

Figure S7. Comparison of the adsorption and heat characteristics of JLHA at initial pH 4.0 and pH 5.0 in 0.1 mol/L KNO_3. The top panels depict the bound amounts of carboxylic-Cu (solid red spheres), phenolic-Cu (solid red triangles) and total Cu bound (solid black squares) and the bottom panels the cumulative heat corrected by the heat of background (open black squares) as a function of total amount of Cu^{2+} bound. The symbols in the bottom panels are the experimental data; the red lines (Fit_1) fitted data with an equation that has a similar form to eq 2.

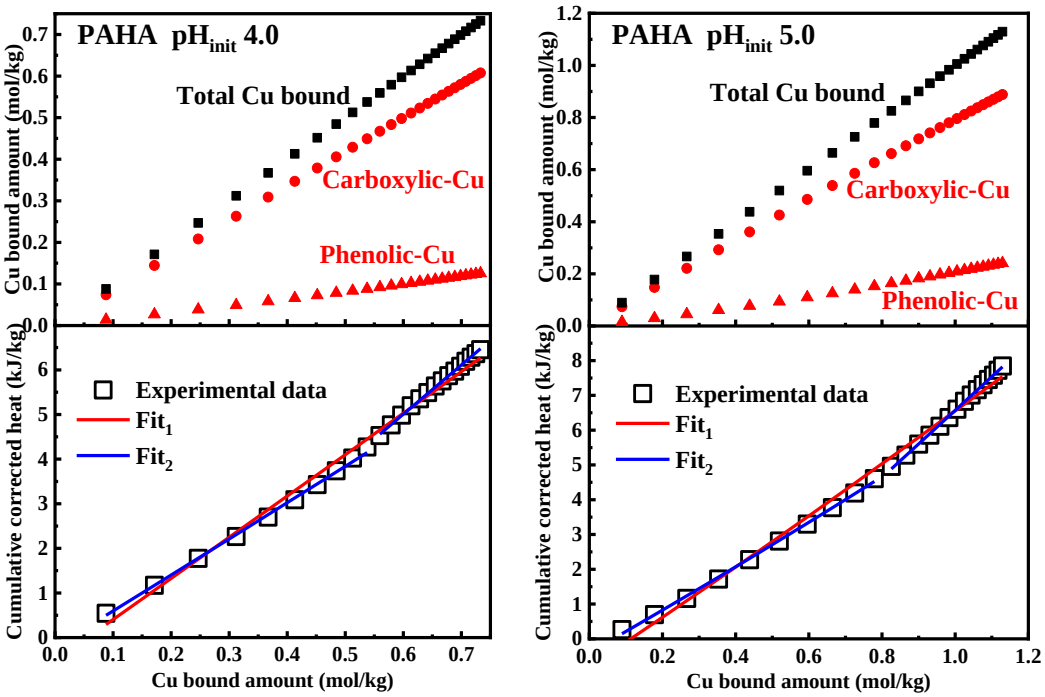

Figure S8. Comparison of the adsorption and heat characteristics of PAHA at initial pH 4.0 and 5.0 in 0.1 mol/L KNO_3. The top panels depict the bound amounts of carboxylic-Cu (solid red spheres), phenolic-Cu (solid red triangles) and total Cu bound (solid black squares), and the bottom panels the cumulative heat corrected by the heat of background (open black squares) as a function of total amount of Cu^{2+} bound to PAHA. The symbols in the bottom panels are the experimental data; the red lines (Fit_1) fitted data with an equation that has a similar form to eq 2. The blue lines (Fit_2) are refined fitted data with an equation similar to eq 2 that are fitted by making a difference between low and high Cu loadings.

References

1. Koopal, L. K.; Riemsdijk, W. H. V.; Wit, J. C. M. D.; Benedetti, M. F. Analytical isotherm equations for multicomponent adsorption to heterogeneous surfaces. *J. Colloid Interface Sci.* **1994**, *166* (1), 51-60.
2. Koopal, L. K.; Van Riemsdijk, W. H.; Kinniburgh, D. G. Humic matter and contaminants. General aspects and modeling metal ion binding. *Pure Appl. Chem.* **2001**, *73* (12), 2005-2016.
3. Benedetti, M. F.; Milne, C. J.; Kinniburgh, D. G.; Riemsdijk, W. H. V.; Koopal, L. K. Metal ion binding to humic substances: application of the Non-Ideal Competitive Adsorption Model. *Environ. Sci. Technol.* **1995**, *29* (2), 446-457.
4. Kinniburgh, D. G.; Milne, C. J.; Benedetti, M. F.; Pinheiro, J. P.; Filius, J.; Koopal, L. K.; Van Riemsdijk, W. H. Metal Ion Binding by Humic Acid: Application of the NICA-Donnan Model. *Environ. Sci. Technol.* **1996**, *30* (5), 1687-1698.
5. Koopal, L. K.; Saito, T.; Pinheiro, J. P.; Riemsdijk, W. H. V. Ion binding to natural organic matter: General considerations and the NICA–Donnan model. *Colloids Surf., A* **2005**, *265* (1–3), 40-54.
6. Nederlof, M. M.; Wit, J. C. M. D.; Riemsdijk, W. H. V.; Koopal, L. K. Determination of proton affinity distributions for humic substances. *Environ. Sci. Technol.* **1993**, *27* (5), 846-856.
7. Tan, W.; Xiong, J.; Li, Y.; Wang, M.; Weng, L.; Koopal, L. K. Proton binding to soil humic and fulvic acids: experiments and NICA-Donnan modeling. *Colloids Surf., A* **2013**, *436*, 1152-1158.
8. Xu, J.; Tan, W.; Xiong, J.; Wang, M.; Fang, L.; Koopal, L. K. Copper binding to soil fulvic and humic acids: NICA-Donnan modeling and conditional affinity spectra. *J. Colloid Interface Sci.* **2016**, 473, 141-151
9. Smith, R.; Martell, A.; Motekaitis, R. NIST standard reference database 46. NIST *Critically Selected Stability Constants of Metal Complexes Database*, version 8; NIST: Gaithersburg, MD, 2004; 2.
10. Cabaniss, S. E.; Maurice, P. A.; Madey, G. A stochastic model for the synthesis and degradation of natural organic matter. Part III: Modeling Cu(II) complexation. *Appl. Geochem.* **2007**, *22* (8), 1646-1658.